Vanadium States in Doped Bi₁₂SiO₂₀

Petya PETKOVA *, Petko VASILEV, Mustafa MUSTAFA, Ivaylo PARUSHEV

Shumen University "Konstantin Preslavsky", 115 Universitetska Street, 9712 Shumen, Bulgaria

We have investigated the absorption of the V doped $Bi_{12}SiO_{20}$ in the spectral region $1.45 - 2$ eV ($11\ 696 - 16\ 129$ cm^{-1}). The observed absorption bands are due to the V^{2+} and V^{3+} ions in the same spectral region. These absorption bands do not contain information about the exact energy position of the vanadium levels. Therefore, we have calculated the second derivative of absorption. It is established that all vanadium ions are surrounded by distorted octahedral coordination in $Bi_{12}SiO_{20}$ (BSO). The energy level structures of the vanadium ions in BSO are also presented. We have calculated the field parameters Dq and the Racah parameters B and C for V^{2+} ion. We have determined the field parameters Dq, Ds and Dt for V^{3+} ion.

Keywords: vanadium doped sillenites, oxygen tetrahedron, Racah parameters, Jahn-Teller effect, spin-orbit interaction.

1. INTRODUCTION

Sillenite-type $Bi_{12}SiO_{20}$ (BSO) pure and doped single crystals are widely used in optical devices, spatial – time light modulators and as holographic media [1, 2]. BSO are cubic crystals, I23 space group symmetry, built up of Si–O₄ tetrahedrons and deformed Bi–Oₙ polyhedrons [3], defined by some authors as Bi–Oₙ (n = 7) – octahedrons [4] or as Bi–O – pseudo-octahedrons [5]. The chemical bonds Bi–O and Si–O in BSO are covalent [3]. The primitive cell consists of 24 atom of Bi, 2 atom of Si and 40 atom of O. At room temperature the band – gap of non-doped BSO crystal is about 3.2 eV. It has a yellow color that comes from the broad absorption shoulder below the actual band edge attributed to bismuth antisite defect [6]. The performance of BSO photorefractive materials could be improved by adding transition metal series ions. These might help to optimize the material characteristics like photorefractive sensitivity, speed of the charge transport, life time of the carrier trapping, etc.

After reported literature data most of doping ions in BSO are placed at metal position in Si–O₄ – tetrahedron [7]. For Ru, Cu and Mn ions there are data for occupation of both metal positions in tetrahedron (replacing Si) and in pseudo octahedron (replacing Bi) [5, 7, 8].

The optical properties of sillenites depend mainly on their structural defects [2]. The defects in the sillenites can be generated in several ways:

a) – by thermo-chemical influence.

After annealing in oxygen environment, O(3) – empty positions are filled and the crystals are lightening. The opposite occurs during the annealing in vacuum. Bi³⁺– ions occupy the tetrahedral positions and they give yellow colour to the crystals (presence of O(3) empty positions is another hypothesis for explaining the yellow colour of undoped sillenites).

b) – by the inclusion of impurities during the grown without changing the stoichiometry of the melt.

This is the main method of generating defects in the crystal structure. Thus some parameters of the crystals can change in some direction by appropriate doping. The sillenites can be doped easy and a little change in the concentration of dopants can dramatically change their optical properties and photoconductivity.

The dopants in the sillenites occupy tetrahedral and octahedral positions and they can:

– replace existing empty crystal positions in advance of the metal Si – atom.

– displace the ion which stabilizes the X – dopant (X = Al, P, Ag, Mn, Cr etc.).

– replace Bi³⁺ – ion which has taken the place of Si – atoms in SiO₄ tetrahedron.

The authors of [9] report that the Bi⁰_M defect should be dominant in the illuminated state of the $Bi_{12}MO_{20}$ and should act simultaneously as a donor and an acceptor. Under proper excitation it can create traps for electrons (Bi⁺_M) and holes (Bi⁻_M) throughout the lattice, the basic conditions required for optical recording via space – charge modulation. The model explains the domination of paramagnetic defects in the illuminated and diamagnetic defects in the unnealed state, and accurately reproduces conditions that are necessary to transform the illuminated state predicts the formation of the broad and intense shoulder below the optical absorption edge of the BMOs, explaining their coloration under appropriate illumination.

The doping elements can have the same or different valence of the ions, which are replacing; they can exist in only one stable valence state or in different valence states.

Many studies on the optical absorption coefficient of doped with Al, P, Cr, Mn, Fe, Co, Ni, Cu, Se and Ru sillenites in the visible spectral region have been reported so far and the effect of doping were discussed mainly in respect to possible oxidation states of doping ions, position of allowed electron transitions in the 1.5 eV $– 2.2$ eV region and the dependence of corresponding absorption coefficient on dopant concentration [5, 8, 10 – 18].

Nevertheless, until now there are no systematic complex investigations on doping effects on impurity levels in the band gap (1.45 eV $– 2$ eV). We attempt to

---

*Corresponding author. Tel.: +359-54-830495261; fax: +359-54-830371.
E-mail address: *Petya232@abv.bg* (P. Petkova)

present the effect of doping as well as to specify how vanadium appears itself in the substructures of the sillenites.

2. EXPERIMENTAL DETAILS

We investigated doped BSO crystals with vanadium. All the crystals were grown from stoichiometric melts $Bi_2O_3 : SiO_2 = 6 : 1$ using the Czochralski method in the [001] crystal direction with a low temperature gradient (5 C/cm – 70 C/cm) over the solution. The platinum crucibles that contain the appropriate melt solution were allowed to rotate at 20 rpm. These parameters allow achieving a growth rate of 0.7 mm/h. The same growing conditions were employed for all the samples to achieve an ingots size of height 60 mm and diameter 40 mm with a high degree of homogeneity. The extrinsic carrier concentration of the sample were determined whereas the thickness of the polished crystal plates was measured using a digital micrometer. The starting materials Bi_2O_3, SiO_2 and V_2O_5 are used with a high purity of 99.999 %.

The concentration of doping was determined by flame (Zeeman 3030) and electrical – thermal atomic (Varian 240) absorption spectrometry as well as by inductively coupled plasma atomic emission spectrometry (Jobin Yvon, ULTIMA 2).

The vanadium ions are situated in the places of Bi^{3+} ions in BiO_6 octahedrons and the other part of the sillenite structure consists of SiO_4 tetrahedrons [19]. The concentration of vanadium in the crystal lattice is 3.31×10^{18} cm^{-3}. The shearing cut of the samples is (100). The plates have polished surfaces and their thickness is 1 mm.

Optical radiation interacts with materials in a variety of ways depending upon the material and the wavelength of the optical radiation – giving rise to the optical spectra, which could be either emission or absorption spectra in solids, normally it is the absorption spectra, which is observed. This is nothing, but the variation of the radiation intensity as a function of wavelength. Study of the absorption spectra of transition metal ions embedded in solids had been extensively used to obtain information about the local symmetry in which the ion sits in its valence state, its site preference and determination of the degree of covalence of the metal – ligand bond.

The experimental set up for measurement of the absorption coefficient in the visible and near IR region consists of the following: a halogen lamp with a stabilized 3H-7 rectifier, a SPM-2 monochromator, a system of quartz lenses, a polarizer, a crystal sample holder, and a Hamamatsu S2281-01 detector.

The absorption coefficient is calculated using the formula: $\alpha = (1/d)\ln(I_0/I)$ (1), where I_0 is the intensity of the incident light, I is the intensity of the passing light and d is the sample thickness.

3. RESULTS

We measured absorption spectra of $Bi_{12}SiO_{20}$ and $Bi_{12}SiO_{20}$:V in the spectral region 1.45 eV – 2 eV (Fig. 1, Fig. 2, a, Fig. 3, a). It is seen that the vanadium structure is complicated and its shape does not give information about

the number of the electron transitions in V^{2+} and V^{3+} ions.

Therefore, the calculation of the first derivative of the absorption coefficient gives information about the number of the electron transitions in the investigated vanadium complexes (Fig. 2, b, Fig. 3, b). The exact energetic position of the electron transitions in the vanadium ion is determined by calculation of the second derivative of the absorption coefficient (Fig. 2, c, Fig. 3, c). The Jahn-Teller effect manifests as distortion of the oxygen – octahedra of V^{2+} and V^{3+}. The final result is the lower symmetry C_{4v} (Fig. 4, a and b).
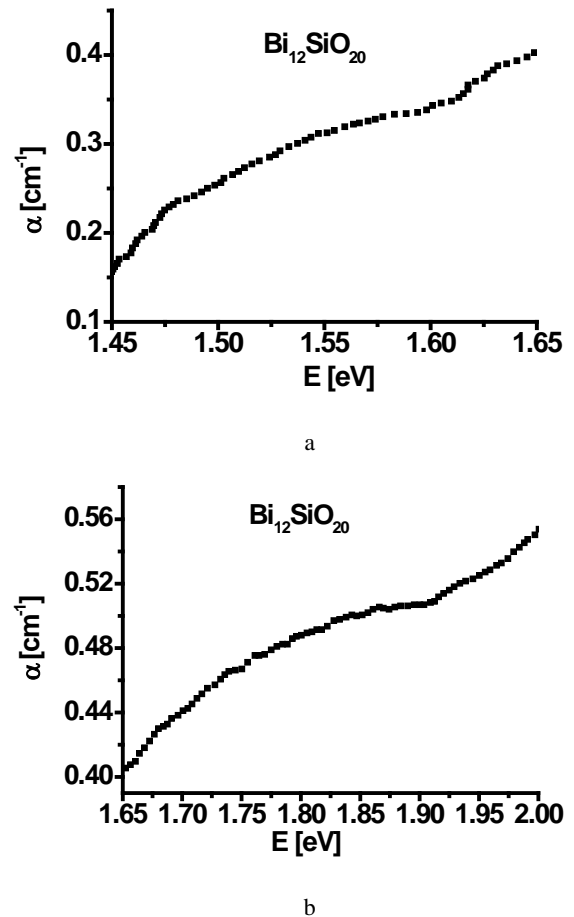

a

b

Fig. 1. Absorption spectrum of $Bi_{12}SiO_{20}$ in the spectral regions: a – 1.45 eV – 1.65 eV; b –1.65 eV – 2 eV

## 4. DISCUSSION

In this section, we describe our crystal – field model for the V^{2+} and V^{3+} centers in $Bi_{12}SiO_{20}$ without the presence of V^{5+} ions. Vanadium 5+ has a d^0 electronic configuration and will not have any d – d optical transitions. However, d^0 ions can contribute to optical transitions if there is a charge – transfer process. Charge – transfer transitions are usually high energy transitions which are predicted by molecular orbit theory, but not by crystal field theory. These high-energy transitions promote electrons that mainly belong to states of ligand ions to states that mainly belong to the transition metal ion [20]. Charge – transfer transitions of V^{5+} in various glass and crystal hosts all occur in or around the UV region [21 – 23]. Since the optical transitions observed for vanadium doped BSO occur at lower energies they are not attributed to a charge – transfer transition. Therefore
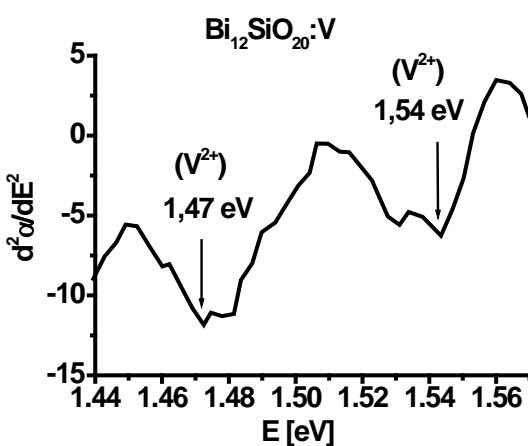
V^{5+} is not believed to contribute to any observed optical transition of BSO : V.
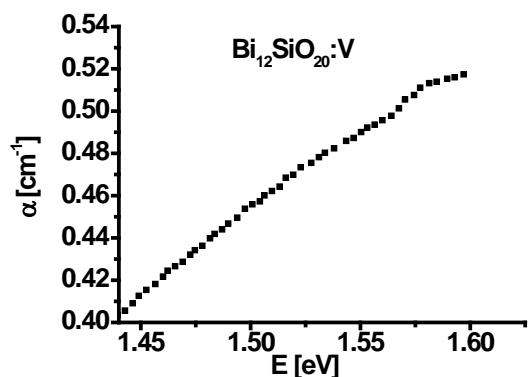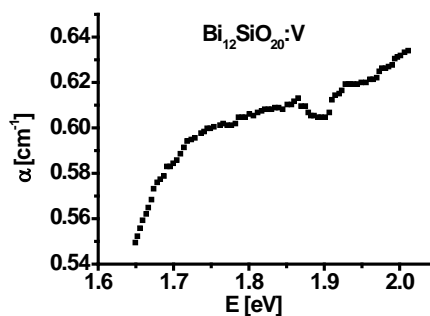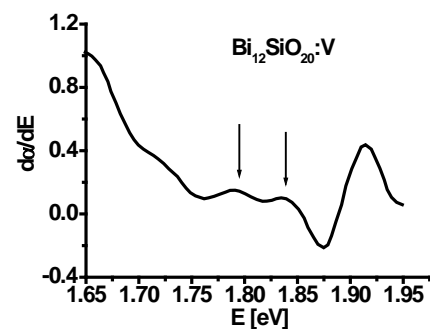

a
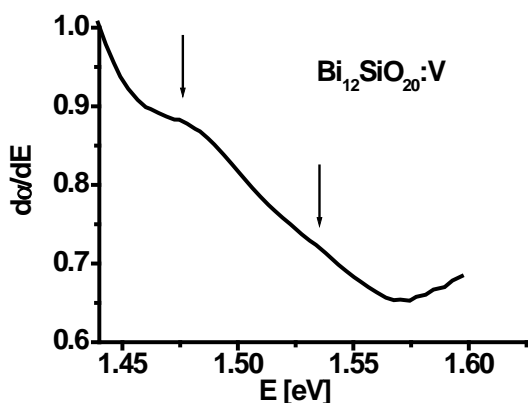
b

c

Fig. 2. Absorption spectrum (a) of $Bi_{12}SiO_{20}$:V in the spectral region 1.45 eV – 1.65 eV; b – calculated first derivative of absorption coefficient; c – calculated second derivative of absorption coefficient

The assignment of the EPR signals to octahedral V^{4+} is usually supported on the detection of the signal at room temperature, since, in general, it is admitted that tetrahedral V^{4+} is observable only at low temperature due to relaxation effects [24]. The presence of V^{4+} at room temperature shows that the actual spin – lattice relaxation times of this ion depend critically on the energy of the first excited state,
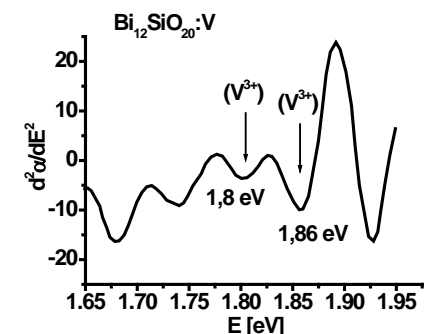
which increases with site distortion, because of increasing splitting of the $e(d_{x^2-y^2}, d_{z^2})$ level, which is degenerate in ideal tetrahedral symmetry [25].

a

b

c

Fig. 3. Absorption spectrum (a) of $Bi_{12}SiO_{20}$:V in the spectral region 1.65 eV – 2 eV; b – calculated first derivative of absorption coefficient; c – calculated second derivative of absorption coefficient

We expect the manifestation of V^{4+} when the doped crystal will be illuminated with UV light. In this case, the process $V^{3+} - e^- \rightarrow V^{4+}$ will be realized. The presented model includes a full treatment of the C_{4v} crystal field which acts upon the vanadium ion. The V^{2+} impurity in BSO has the d^3 configuration and the V^{3+} has d^2 configuration. The crystal – filed potential consists of the field of O_h symmetry. This means that the octahedral coordination about the vanadium ion has six oxygen ions.

It is shown in the literature that when the V^{2+} ion is in the octahedral oxygen coordination the electron transition $^4A_2(F) \rightarrow {}^4T_2(F)$ observes at 1.47 eV (11 848 cm^{-1}) and 1.54 eV (12 422 cm^{-1}) for different materials [19]. In our case, we observed these two transitions for BSO : V (Fig. 2, c). The other two electron transitions at 1.8 eV

($\Delta_2 = 14\,514$ cm^{-1}) and 1.86 eV ($\Delta_3 = 14\,993$ cm^{-1}) correspond to the V^{3+} ions in the bismuth position (Fig. 3, c) [19].

The Tanabe-Sugano model takes into account the interactions between two or more 3d electrons in the presence of a crystal field.
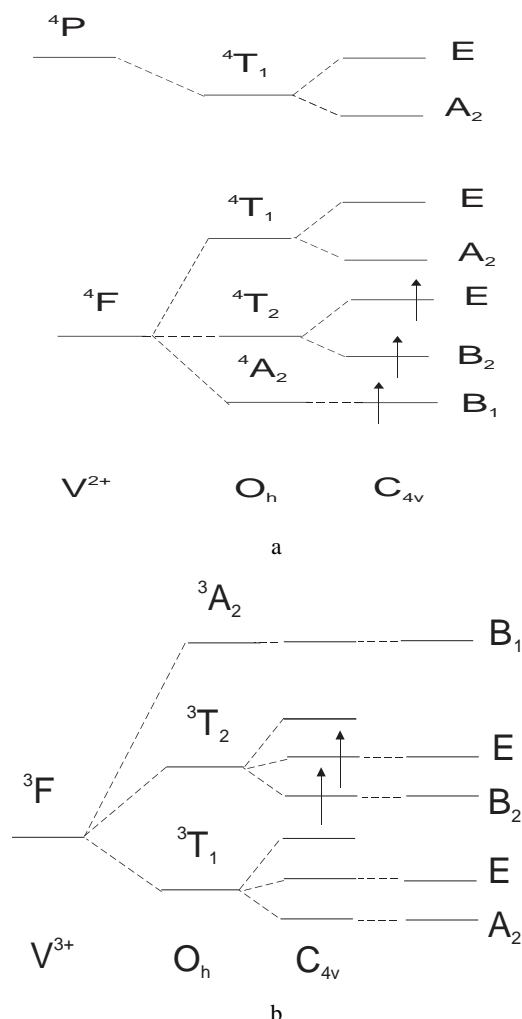
Fig. 4. Energy diagram of V^{2+} ion (a) and V^{3+} ion (b) in C$_{4v}$ symmetry

The free ion states are shown on the far left of a Tanabe-Sugano diagrams where ($Dq/B = 0$). The free ion states are governed by electron–electron interactions and so are labelled by $2S + 1L$ states (also called L–S terms), where S is the total spin angular momentum and L is the total orbital angular momentum [20]. The energy separation between the various $2S + 1L$ states is given in terms of the Racah parameters (A, B and C). These parameters describe the strength of the electrostatic interactions between multiple 3d electrons [26]. Tanabe and Sugano calculated the energy matrices for each state of 3d^2 to 3d^5 ions in an ideal octahedral crystal field [27], their derivation was subsequently verified elsewhere [28]. These energy matrices can then be used to calculate how the $2S + 1L$ free ion levels split up, and vary, as a function of the ratio between the crystal field strength and the inter-electronic interaction (measured in Dq/B). Tanabe-Sugano diagrams take advantage of the fact that C/B is almost independent of atomic number and the number of

electrons, for all first row transition metal elements, $C/B = 4 – 5$ [26].

In these diagrams, the term $^3T_1$ of the lowest energy level ^3F has the value of energy $E(^3T_1(^3F)) = 7.5B + 15Dq - 0.5$ sqrt $(225B^2 – 180DqB + 100Dq^2) = 11\,140$ cm$^{-1} = \Delta_1$, where $B = 1272$ cm^{-1} and $Dq = 2951$ cm^{-1}. Two ligand field parameters are introduced because of the presence of an addition axial field: the Ds parameter which is the second order radial integral and the Dt parameter which is the fourth order radial integral related to Dq. The final result of Jahn-Teller effect gives the following three equations: $\Delta_1 = –3Ds + 5Dt$, $\Delta_2 = 10Dq + 4Ds + 5Dt$ and $\Delta_3 = –4Ds – 5Dt$. Thus, the parameters Ds and Dt have values respectively –3733 cm^{-1} and –12 cm^{-1}.

The energy–level scheme and transition–selection rules for a transitional ion embedded into a crystal host matrix are determined by the ion valence state, the structure and number of the surrounding ligand ions. Besides, the valence and coordination of the optically active ions, the quality of the crystals often determine the potential laser application. In the static crystal field approach each ion is assumed to be fixed at a mean lattice position and the crystal field experienced by a centre will reflect the symmetry of its environment.

The bond between the vanadium ion and the surrounding ligands is covalent. This covalence reduces the positive charge of the metal ion as a result of the inductive effect of ligands [29]. The reduction of the positive charge of the vanadium ion leads to an increase in the radial extension of the d-orbitals. Thus, the electron–electron repulsions weaken and the energy of the state 4P decreases. The influence of the covalence leads to the reduction of the difference in the energies between the states ^4F and ^4P in the vanadium complex. This difference is less in comparison with the difference in the same energies of the gaseous ion. The lowering of the level ^4P determines the magnitude of the covalence. This effect is famous as Nephelauxetic. Sometimes it is expressed by the parameter $\beta_0 = [(B – B') / B]\cdot 100$, where B is the Racah parameter for the free ion and $B' = 887$ cm^{-1} is the same parameter for the complex [30]. β_0 shows the percentage of the energetic decrease of the state ^4P for V^{2+}. The calculations show that $\beta_0 = 16$ %. This means that the Jahn-Teller effect is stronger. The equation $Dq^2 = (18B^2 + 3B)/8$ is the result of the transformation of the matrix of the energies $^4T_1(^4F)$ and $^4T_1(^4P)$. The value of the crystal field parameter Dq is 1331 cm^{-1}. The other Racah parameter C is equal to 3992 cm^{-1}.

Clark [31] defined a vanadyl bond as one which has a short bond length in the range 1.57 Å – 1.68 Å; it is a multiple bond with a π-component arising from electron flow from O(pπ) to V(dπ) orbitals. When there are two vanadyl bonds present in a polyhedron, they are in a cis arrangement [32]. This cis arrangement for metals with d electrons is preferred over the trans arrangement because the strongly π-donating O ligands then share exclusively one dπ orbital each (d_{xz}, d_{yz}) and share a third (d_{xy}), whereas in the trans configuration, they would have to share two dπ orbitals and leave one unused [33].

The literature [34] informs us of the Nephelauxetic parameter $\beta = B(\text{complex}) / B(\text{free ion})$. If the value of β is

in the interval $0.54-0.81$, it manifests the metal ligand σ bond. In the case of vanadium doped BSO the ligand bond is π, because $\beta = 1.16$.

The spin–orbit coupling constant $\lambda = 150 \text{ cm}^{-1}$ for (V^{2+}) [35]. The spin–orbit parameters for the examined vanadium tetrahedrons are as follow: $S = 3/2$, $J = 1/2$; $3/2$ and $L = 0$; 1. The contribution of the spin–orbit interaction in the energy of each level is expressed as $E = (1/2)\lambda[J(J + 1) - L(L + 1) - S(S + 1)]$ [12]. Therefore, $E_{J=1/2, L=0} = 225 \text{ cm}^{-1} = 1.5\lambda$, $E_{J=1/2, L=1} = 375 \text{ cm}^{-1} = 2.5\lambda$ and $E_{J=3/2, L=1} = 150 \text{ cm}^{-1} = \lambda$ for the vanadium–oxygen complex in $Bi_{12}SiO_{20}$. The difference between the energies of two neighbouring states arising due to the spin–orbit interaction is determined by the expression $\Delta E_{J, J+1} = \lambda(J + 1)$ [36]. Thus, $\Delta E_{1/2, 3/2} = 225 \text{ cm}^{-1}$ and $M_S = 3/2$, $M_L = 0$, ± 1.

5. CONCLUSIONS

In this work, the interesting fact is that the impurity absorption structure in the visible spectral region for $Bi_{12}SiO_{20}$ is characteristic for V^{2+} and V^{3+}. This is important for the investigation of defects in the cubic crystals and glasses in the magnetic field and this will help for the application of BSO:V in holography. In the case of V doped BSO the ligand bond is π. Jahn-Teller effect is stronger than the spin-orbit interaction in the tetrahedral complex of V^{2+}.

REFERENCES

1. **Gunter, P., Huignard, J.** Photorefractive Materials and Their Applications. Part 1. Springer Science + Business Media, New York, 2006.
http://dx.doi.org/10.1007/b106782

2. **Gunter, P., Huignard, J.** Photorefractive Materials and Their Applications. Part 2 and 3. Springer Science + Business Media, New York, 2007.

3. **Mihailova, B., Gospodinov, M., Konstantinov, L.** Raman Spectroscopy Study of Sillenites. I. Comparison between $Bi_{12}(Si,Mn)O_{20}$ Single Crystals *Journal of Physics and Chemistry of Solids* 60 1999: pp. 1821–1827.
http://dx.doi.org/10.1016/S0022-3697(99)00194-8

4. **Marinova, V., Veleva, M., Petrova, D.** Optical Properties of $Bi_{12}SiO_{20}$ Single Crystals, Doped with 4d and 5d Transitions Elements *Journal of Applied Physics* 89 (5) 2001: pp. 2686–2689.

5. **Ramaz, F., Rakitina, L., Gospodinov, M., Briat, B.** Photorefractive and Photochromic Properties of Ruthenium-doped $Bi_{12}SiO_{20}$ *Optical Materials* 27 2005: pp. 1547–1559.
http://dx.doi.org/10.1016/j.optmat.2004.11.007

6. **Oberschmid, R.** Absorption Centers of $Bi_{12}GeO_{20}$ and $Bi_{12}SiO_{20}$ Crystals *Physica Status Solidi* 89 (1) 1985: pp. 263–270.
http://dx.doi.org/10.1002/pssa.2210890128

7. **Kargin, Y., Burkov, V., Maryin, A., Egorysheva, A.** Kristally $Bi_{12}M_xO_{20-\delta}$ so strukturoi sullenita. Sintez, stroenie, svoistva (Sillenite $Bi_{12}M_xO_{20-\delta}$ Crystals: Synthesis, Structure, and Properties). Moscow: Institute of General Inorganic Chemistry, RAS, 2004 (in Russian).

8. **Marquet, H., Tapiero, M., Merle, J., Zielinger, J., Launay, J.** Determination of the Factors Controlling the Optical Background Absorption in Nominally Undoped and Doped Sillenites *Optical Materials* 11 (1) 1998: pp. 53–65.

9. **Lima, A., Lalic, M.** First-principles Study of the Bi_MMO_4 Antisite Defect in the $Bi_{12}MO_{20}$ (M = Si, Ge, Ti) Sillenite Compounds *Journal of Physics: Condensed Matter* 25 2013.

10. **Nechitailov, A., Krasinkova, M., Mokrushina, E., Petrov, A., Kartenko, N., Prokofiev, V.** Impurity Defects in Cr-doped $Bi_{12}SiO_{20}$ and $Bi_{12}TiO_{20}$ Crystals *Inorganic Materials* 36 (8) 2000: pp. 820–825.
http://dx.doi.org/10.1007/BF02758604

11. **Egorisheva, A., Burkov, V., Kargin, Yu., Vasiliev, A., Volkov, V., Skorikov, V.** Spectroscopic Characteristics of $Bi_{12}SiO_{20}$ and $Bi_{12}TiO_{20}$ Crystals Doped with <Mn>, <Mn, P>, <Cr, P>, <Cr, Ga> and <Cr, Cu> *Inorganic Materials* 37 (8) 2001: pp. 965–973.

12. **Burkov, V., Egorisheva, A., Kargin, Yu.** Electron Configuration and Optical Spectra of Tetrahedral $[MO_4]^{n-}$ Complexes of 3d Elements *Journal of Inorganic Chemistry* 48 (4) 2003: pp. 620–638.

13. **Marinova, V., Lin, S., Hsieh, M., Liu, R., Hsu, K.** Photorefractive Materials, Effects and Devices PR'09, P1 – 39, 2009.

14. **Egorisheva, A., Volkov, V., Coya, C., Zaldo, C.** Tetrahedral Cr^{4+} and Cr^{5+} in $Bi_{12}TiO_{20}$ Single Crystals *Physica Status Solidi (b)* 207 (1) 1998: pp. 283–288.

15. **Potera, P., Pircuch, A.** Color Centers in Cu-doped $Bi_{12}SiO_{20}$ Crystals *Physica B* 387 (1–2) 2007: pp. 392–395.

16. **Kovacs, L., Capelli, R., Gospodinov, M.** Vibrational Frequencies of the Impurity – centred Oxygen Tetrahedra in Sillenites *Vibrational Spectroscopy* 46 (1) 2008: pp. 69–75.

17. **Zmija, J., Malchowski, M.** Photochromic Effects in Sillenite Single Crystals *Archives of Materials Science and Engineering* 33 (2) 2008: pp. 101–106.

18. **Ahmad, I., Marinova, V., Goovaerts, E.** Photorefractive Materials, Effects and Devices PR'09, P1 – 38, 2009.

19. **Lever, A.** Inorganic Electronic Spectroscopy. Toronto, 1984.

20. **Garcia-Sole, J., Bausa, L., Jaque, D.** An Introduction to the Optical Spectroscopy of Inorganic Solids. Wiley, Chichester, 2005.
http://dx.doi.org/10.1002/0470016043

21. **Johnstone, W.** Oxidation Reduction Equilibria in Molten $Na_2O.2SiO_2$ Glass *Journal of the American Ceramic Society* 48 (4) 1965: pp. 184–190.
http://dx.doi.org/10.1111/j.1151-2916.1965.tb14709.x

22. **Belletti, A., Borromei, R., Cavalli, E., Oleari, L.** The Luminescence of VO_4^{3-} Ions in Ca_2PO_4Cl *European Journal of Solid State and Inorganic Chemistry* 35 (6–7) 1998: pp. 483–493.

23. **Brunold, T., Gudel, H., Kaminskii, A.** Optical Spectroscopy of V^{4+} Doped Crystals of Mg_2SiO_4 and Ca_2GeO_4 *Chemical Physics Letters* 271 (4) 1997: pp. 327 – 334.
http://dx.doi.org/10.1016/S0009-2614(97)00466-1

24. **Shiju, N.** Supported Vanadium Oxide Catalysts in Oxidation and Oxidative Dehydrogenation Reactions: Structure and Catalytic Properties. Catalysis Division National Chemical Laboratory, India, 2004.

25. **Vassilikou-Dova, A., Lehmann, G.** Four-valent Vanadium in Vanadinite *American Mineralogist* 74 1989: pp. 1182 – 1185.

26. **Tanabe, Y., Sugano, S.** On the Absorption Spectra of Complex Ions II *Journal of the Physical Society of Japan* 9 1954: pp. 766 – 779.
http://dx.doi.org/10.1143/JPSJ.9.766

27. **Henderson, B., Imbusch, G.** Optical Spectroscopy of Inorganic Solids. Oxford University Press, Oxford, 1989.

28. **Griffith, J.** Theory of Transition Metal Ions. Cambridge University Press, London, 1961.

29. **Drago, R.** Physical Methods in Chemistry. University of Illinois, Urbana, 1981.

30. **Egorisheva, A., Burkov, V., Kargin, Yu., Volkov, V.** Optical Properties of $Bi_{12}TiO_{20}$ and $Bi_{12}SiO_{20}$ Single Crystals Doped with Cobalt *Inorganic Materials* 31 1995: pp. 1087 – 1093.

31. **Clark, R.** The Chemistry of Titanium and Vanadium. Elsevier, New York, 1968.

32. **Evans, H.** Crystal Structure Refinement and Vanadium Bonding in the Metavanadates KVO_3, NH_4VO_3 and $KVO_3 \cdot H_2O$ *Zeitschrift für Kristallographie* 114 1960: pp. 257 – 277.
http://dx.doi.org/10.1524/zkri.1960.114.1-6.257

33. **Cotton, F., Wilkinson, G.** Advanced Inorganic Chemistry. John Wiley & Sons, New York, 1972.

34. **Chandra, S., Gupta, L.** Mass, EPR, IR and Electronic Spectroscopic Studies on Newly Synthesized Macrocyclic Ligand and Its Transition Metal Complexes *Spectrochimica Acta Part A:Molecular and Biomolecular Spectroscopy* 62 (4 – 5) 2005: pp. 1125 – 1130.

35. **Reddy, G., Reddy, R., Reddy, S., Frost, R., Endo, T.** Spectroscopic and Structural Characterization of Pascoite *Spectrochimica Acta Part A:Molecular and Biomolecular Spectroscopy* 79 (5) 2011: pp. 1402 – 1405.

36. **Ballhausen, C.** Introduction to Ligand Field Theory. Mc Graw – Hill Book Company, Inc., New York, 1964.